Electronic Supplementary Material (ESI) for Green Chemistry.

Supplementary Information for

High biomass loadings of 40 wt.% for efficient fractionation to meet biorefinery in solvent aqueous system without adding adscititious catalyst

Hua Zhou, Renli Zhang, Wang Zhan, Liuyang Wang, Lijun Guo, Yun Liu*

* Corresponding author. Email: liuyun@mail.buct.edu.cn or

liuyunprivate@sina.com.cn

Supplementary information includes:

Materials and Methods

Supplementary Text

Figs. S1 to S18

Tables S1 and S3

Full Reference Lists

Materials and methods

Materials

γ-Valerolactone (≥98%) and cellulase (from *Trichoderma longibrachiatum*, ≥1.0 U/mg) were purchased from Sigma-Aldrich Co. (St. Louis, MO, USA). Tetrahydrofuran (≥99.5%), ethanol (≥99.7%), methanol (≥99.5%), acetone (≥99.5%), acetonitrile (≥99.9%) and ethyl acetate (≥99.5%) of analytic grade were bought from Beijing Chemical Factory (Beijing, China). Dioxane (≥99%) and acetic acid (≥99.8%) of analytic grade were purchased from Aladdin Industrial Co. Ltd (Shanghai, China). The standards of glucose (99.5%) and ethanol (99.5%) of chromatographic grade were bought from Guangfu Fine Chemical Co. Ltd., (Tianjin, China). The standards of 5-(hydroxymethyl) furfural (5-HMF, 99%) and levulinic acid (99%) of chromatographic grade were purchased from J & K Scientific GmbH (Pforzheim, Germany). An industrial thermo-tolerant yeast strain, *S. cerevisiae,* was purchased from Angel Yeast Co., Ltd., (Yichang City, Hubei province, China). All other regents used in this work of analytic grade were bought in Beijing locate markets, China.

Irradiation pretreatment of lignocellulose

Two kinds of lignocellulose biomass were tested in this work: (I) Agricultural waste biomass: Reed stover and corncob were gifted from the Hunan Irradiation Center (Hunan, Chian), bagasse was obtained in Beijing location (China); (Π) plant woods: Eucalyptus hardwood and pine softwood were obtained from the forest products (Guangxi Gaofeng Forest, China). A batch of dry biomass materials in sealed small test casket (40 cm (length) ×18 cm (width)×15 cm (Height)) was

irradiated at room temperature at a ^{60}Co-γ radiation source intensity of 9.99×10^{15} Bq in the Hunan Irradiation Center (Changsha city, Hunan province, China). The irradiation procedures of biomasses were detailed in our previous work (20). Based on previous experimental data, the specific level of γ-irradiation dose was selected as 800 kGy in this work. After irradiation pretreatment, the irradiated biomass was grounded in DFY-1000 pulverizer (Wenlin, Zhejiang, China) for 30 seconds and sieved by 60 meshes, after which was conducted to fractionate in green solvent aqueous systems, which consists of 40 wt. %γ-Valerolactone (GVL) and 60 wt. % water (40:60, GVL/H_2O). The components of tested biomass feedstocks before and after irradiation treatment are given in Supplemental Table S1. Excitedly, we obtain finer particle size distributions of grinded biomass and 3- or 4- fold less energy consumption in the batch crushing operational unit for the irradiated biomass *versus* untreated samples (Fig. S1). It is indicated that irradiation assisted treatment is probably belonged to an energy consumption competitive process, which is very critical for lignocellulose biorefinery.

Fractionation of irradiated biomass in organic solvent/water system

An overview scheme of biomass fractionation via irradiated assisted in green aqueous systems is depicted in Fig. S2. 1.0 g of irradiated biomass along with 10 mL mixture co-solvents was loaded into 15 mL high pressure stainless steel (Beijing, China, tolerance pressure 3 MPa) and placed into an oil bath with a magnetic digital stirring hotplate (Gongyi, Henan, china). The mixture was stirred by a magnetic stir bar in the reactor at 1000 rpm and 170 °C. After 1 h reaction, the reactor was

immediately cooled to below 60 °C by placing it in cold water pool. The reaction mixture was filtered using 0.45 μm filter paper to separate the solids residue and the filtrate. The solid residue, named as cellulose fraction, was washed three times with 10 mL reaction reagents and then dried in oven at 60 °C for 48 h. The filtrate and eluent derived from washing solid residue cellulose were combined together and diluted 5-fold with ultrapure water to precipitate lignin fraction. Through 10,000×g centrifugation for 15 min, supernatant and precipitate were obtained. The supernatant fraction was mainly composed of hemicellulose hydrolysate (including C5 and C6 monomeric and oligomers). The precipitate was expressed as lignin fraction. The untreated biomass was conducted with the same protocol described above as the blank control. Yields of each fraction obtained and their components were calculated. Using ball milling treatment instead of irradiation assisted process, we achieve bad fractionation efficiency of biomass in the same green aqueous system (Fig. S3). Compared with the untreated biomass, ball milling treatment has no positive effect on fractionation efficiency. The key for high efficiency of irradiation assisted process is due to active acid sites mediated from irradiation, which is helpful to cellulose enzymatically conversion to sugars (Fig. S4). To screen the most suitable organic solvent/water systeme for biomass fractionation, seven different organic solvent/water mixture solutions, including γ-Valerolactone (GVL), tetrahydrofuran (THF), ethanol, methanol, acetone, acetonitrile and dioxane, were evaluated in this work. The weight ratio of organic solvent to water was fixed at 80:20. The results of Fig. S5 show that GVL/H_2O and THF/H_2O systems possess the predominant fractionation efficiency of

biomass among the tested seven different mixture solutions. Furthermore, the effects of weight ratios of solvent to water for GVL/H_2O and THF/H_2O systems on biomass fractionation were tested (Seen in Fig. S6 and Fig. S7).

Parameters optimization of biomass fractionation in 40:60 GVL/H_2O

We further optimized three primary factors affecting fractionation efficiency of biomass in GVL/H_2O mixture solutions as the functions of reaction time (1 h, 2 h, 3 h and 4h) (Fig. S8), reaction temperature (110 °C, 130 °C, 150 °C, 170 °C and 190 °C) (Fig. S9), and biomass loading (10 wt. %, 18 wt. %, 25 wt. %and 40 wt. %) (Fig. S10). The reaction was conducted in 15 mL high pressure stainless steel (Beijing, China, tolerance pressure 3 MPa) putting into an oil bath heated to designed temperature with a magnetic digital stirring hotplate (Gongyi City Yuhua Instrument Co., Ltd.，china). The mixture was stirred by a magnetic stir bar in the reactor at 1000 rpm. It is appealing that biomass fractionation can be conducted at high biomass loadings of 40 wt.% through irradiated assisted in 40:60 GVL/H_2O, which can achieve more soluble sugars and lower operational cost. Only using water as solution, we cannot obtain cellulose and lignin fractions although the C5 and C6 concentration in hydrolysate increase continuously with increasing reaction time (Fig. S5). However, based on the kinetic curves (Fig. S11) of biomass hydrolysis in water, we observe that the irradiated lignocellulose is prone to thermo-hydrolysis at 170 °C than untreated sample.

Aqueous phase separation and GVL recycle

A given volume of ethyl acetate (EAC) was added to the liquid solutions resulting

from high pressure stainless steel fractionation reactor using 40:60 GVL/H_2O mixtures to create a separate aqueous phase. The final volume of EAC was equivalent to GVL volume. The mixtures were poured into a 150 ml glass funnel with stopper and kept it stand for 1 h. The heavier aqueous phase and the lighter GVL-rich phase extracted by EAC were obviously achieved and separated. After that, the sugar monomers and oligomers compositions in the aqueous phase were analyzed. Once recovering EAC by vacuum distillation at -0.1 MPa and 50 °C, the GVL-rich stream contained 99.6 wt. % of original GVL and 2% acetic acid (which is derived from hemicellulose in the reaction) could be re-used in the next batch for biomass fractionation. After 5 batches recycles, even higher C5 and C6 concentrations in hydrolysis aqueous phase as well as similar yields of cellulose and lignin fractions were obtained in comparison with those obtained with fresh GVL, demonstrating that the limited formation of by-products had no detrimental effect on the biomass fractionation efficacy of GVL (Fig. S12).

Cellulose fraction biologically upgrading to ethanol

To examine the upgrading bioconversion of the obtained cellulose solid residue with high Crl value, analyzed by XRD (Fig.S13), to ethanol using simultaneously saccharification and fermentation (SSF), a designed amount of cellulase (20 mg protein/g glucan) and 0.5 mL *Saccharomyces cerevisiae* stock broth (OD600=~6) were added into 50 mL Erlenmeyer flask supplemented with 10 mL fermentation media consisted of cellulose fraction loadings (15 wt%) and nutrition substrates (yeast extract 30 g/L, peptone 50 g/L, $CaCl_2$ 2.5 g/L, $MgSO_4$ 5 g/L, and citrate buffer 50 mM,

pH 5.0) at 37 °C and 120 rpm in a bed shaker. Erlenmeyer flask was sealed to avoid the oxygen entrance. Samples were periodically taken from the ferments for HPLC analysis of ethanol yield and residue glucose concentration.

Prior to adding yeast inoculated broth and nutrition medium, the cellulose fraction was enzymatically pre-hydrolyzed overnight by cellulase (20 mg protein per g cellulose) under the conditions of 50 °C and 200 rpm. Figure S14 show kinetic curves of glucose enzymatically hydrolyzed by cellulase as the function of time from four different treated lignocellulose (using reed stover as model), including native biomass, irradiation assisted treatment biomass, 40:60 GVL/H_2O solubilization biomass and their synergistic treatment biomass. It appears that the synergistic effects of irradiation assisted and GVL solubilization play a role in enzymatic hydrolysis of biomass to glucose, and nearly 100% glucose yields can be achieved after 60 h hydrolysis by 20 mg even 10 mg cellulase per g cellulose. We also examine the yields of total soluble sugars and monomeric glucose by enzymatic hydrolysis (10 mg protein per g cellulose) from different cellulose types separated through IASC in 40:60 GVL/H_2O (Fig. S15). Furthermore, the effects of cellulose loadings on the yields of monomeric glucose are also evaluated when it is fixed the enzymes loadings at 20 mg protein per g cellulose (Fig. S16).

In addition, the toxicity of limited GVL (~1 wt. %) left in aqueous phase on the activities of cellulase and xylase as well as the *S. cerevisiae* yeast growth curve was tested. It reveals that limited GVL (~1 wt. %) shows no depressive effects even GVL content up to 4 wt. % in an aqueous phase has no detrimental influence on activities

of cellulase and xylase as well as the *S. cerevisiae* yeast growth (Fig. S17).

Hemicellulose hydrolysis fraction Chemical upgrading to furans

0.15 mM of $AlCl_3$ (Sigma-Aldrich) was added into a 15 ml thick-walled glass reactor (China) supplement of 1.5 g reed stover aqueous phase solution (expressed as hemicellulose hydrolysis fraction) separated through EAC extraction from 40:60 GVL/H_2O reaction. To begin the reaction, the resulting mixture was placed in an oil bath heated with a magnetic digital stirring hotplate (Gongyi, Henan, China). This hotplate was used to stir a magnetic stir bar in the reactor at 1,200 rpm. After desired reaction time, the reactor was immediately cooled by placing in a cold water pool. Once adding a given amount of sodium chloride into the mixture reaction, the heavier aqueous phase and lighter organic phase was separated and removed using a syringe and needle to measure its mass, after which the furfural and 5-Hydroxymethylfurfural (5-HMF) contents of both phases were analyzed by HPLC.

Hemicellulose hydrolysis fraction biological upgrading to microbial lipids

(1) Inoculum cultivation: The strain *Trichosporon cutaneum* CGMMC2.571 was firstly reviving on solid YPD (10 g/ L yeast extract and 20 g/ L peptone and 20 g/ L glucose) agar plate. And then the strain was adapted for xylose metabolism by transferred a single colony into the liquid media consisting of 10 g/ L yeast extract ,20 g/ L peptone and 20 g/ L xylose, incubation at 30 ˚C for 24 h .

(2) Fermentation cultivation and microbial lipids accumulation: The aqueous phase solution separated through EAC extraction from 40:60 GVL/H_2O reactions was directly used as fermentation medium of *T. cutaneum* 2.571 for lipids accumulation.

Due to existing furans in the aqueous phase, detoxification procedure is needed prior to fermentation. $Ca(OH)_2$ overliming detoxification procedure was used in this work [20], which is involved increasing the pH of the hydrolyzates to 11.0 by addition of $Ca(OH)_2$. The pH was held at 20 °C for 20 h. The pH of the detoxified hydrolyzates was then adjusted to pH 6.0, followed by sterilization with 0.2μm filter (PALL Corporation, USA). The final hydrolysate contained 73 g/L total carbon resources(including 9 g/L glucose, 50 g/L xylose and 14 g/L acetate), was used for fermentation at 10% inoculation strain without any nutrient supplement. The fermentation experiments were conducted at 30 °C and 200rpm.

Lipids accumulation during *T. cutaneum* fermentation was visually imaged using Leica DM1000 fluorescence microscopy (Leica Microsystems GmbH, Wetzlar, Germany) after Nile red (≥98.0%, Sigma, DMSO as solvent) dying for 5 min). Neutral lipids (such as triacylglycerols or cholesteryl esters) show yellow–gold emission, and polar lipids (such as phospholipid) show orange/red emission.

(3) Lipid extraction and fatty acid composition analysis by GC-MS: After 145 h fermentation culutre, strain *T. cutaneum* cell was drawn and dried for lipid extraction. Amount of cells was digested with 4M HCl at 78 °C for 1 h before extraction with chloroform/methanol (1:1, v/v) according to the method by Gong et al. (31). Microbial lipid content was expressed as gram lipid per gram cell dried weight (CDW). The lipid coefficient was defined as gram lipid produced per gram substrate consumed. The fatty acid profiles of microbial lipids were determined using a 7890F gas chromatography-mass Spectrometer (GC-MS, Trace ISQ, Thermo Fisher, USA)

after BF_3-methanol methyl esterification according to the method by Gong et al. (33).

Lignin structure analysis by HSQC NMR spectra and gel-permeation chromatography (GPC)

The resulting lignin fraction was precipitated from 40:60 GVL/H_2O solutions during biomass fractionation by addition of 5-fold volume ultrapure water. The structural variances of obtained lignin were characterized by nuclear magnetic resonance (600M NMR) (Bruker, Germany). A molar mass distribution (Mw and Mn) of the lignin element was determined by gel-permeation chromatography (GPC).

Spectroscopy analyses

(1) X-ray diffraction (XRD)

The effects of irradiated assisted treatment and GVL solubilization on the crystallinity index (Crl) of cellulose was performed in a X-ray diffractometer (D8 ADVANCE, Bruker, Germany) using CuKα radiation generated at a voltage of 40 kV and a current of 40 mA. Scans were obtained from 2θ = 5 to 50 with 12- degree steps and 70.8 sec per step. The crystallinity index (CrI) was calculated using the formula given below.

$$Crl = \frac{I_{002} - I_{AM}}{I_{002}}$$

where: ($I_{002} - I_{AM}$) is the signal for the crystalline portion of cellulose. I_{002} is the signal for the total intensity at the location of the crystalline peak portion of cellulose, which in our case was taken at 2θ = 22.9. I_{AM} is the base of the crystalline peak, which is considered to be the contribution by the amorphous cellulose fraction and in our case is taken at 2θ = 18.3.

(2) Transmission electron micr oscope (TEM)

The particle size of the resulting solid cellulose fractions was performed on TEM (H-800, HITACHI, Japan) under ambient conditions. Scanning frequency was from 0.5 to 2.0 Hz.

(3) XPS analysis

Elemental distribution and chemical state on the surface of native and irradiated reed stover was analyzed by X-ray photoelectron spectroscopy (ESCALAB 250, Thermo Fisher Scientific, USA). All the data were acquired using Monochromated Al Kalph (150 W), a pass energy of 200 eV for survey; 30 eV for high resolution scans. The analyzed area was 500 μm×500 μm.

(4) Zeta potential analysis

The surface charge (Zeta potential analysis) of resulted cellulose was determined by measuring the electrophoretic mobility using a Malvern zeta sizer (Malvern instrument, UK).

(5) Nuclear magnetic resonance (NMR)

The resulted lignin precipitated from GVL/H_2O solutions was characterized by HSQC NMR spectroscopy (28). Specifically, lignin (40 mg) were collected directly into the NMR tubes and dissolved in DMSO-d6/pyridine-d5 (4:1, v/v) solutions. NMR spectra were recorded on a 600 MHz Bruker Biospin Avance spectrometer (Billerica, MA) equipped with a cryogenically cooled 5-mm TCI gradient probe with inverse geometry (proton coils closest to the sample). The central DMSO solvent peak was used as internal reference (δC 39.5, δH 2.49 ppm). Volume integration of

contours in HSQC plots used Bruker's TopSpin 3.1 (Mac version) software.

(6) Gel-permeation chromatography (GPC) analysis

The resulted lignin precipitated from GVL/H_2O solutions dissolved in THF (0.05%, w/v) for analysis molecular weight distribution (Mw and Mn) on 1515GPC (Waters, USA) with UV and RI detector. THF was used as eluent and its flow rate was set at 1.0 mL min^{-1}. The column temperature was fixed at 35 °C. The detected molecular weight ranges were 500~4 $\times 10^6$ Da.

Analytical methods of compositions

The cellulose, hemicellulose and lignin contents of lignocellulose biomass were analyzed according to the procedure published by the National Renewable Energy Laboratory (21).

The compositions of aqueous phases, GVL/H_2O, fermentation broth and ethanol/water were analyzed for glucose, xylose, ethanol, acetic acid, GVL, 5-HMF and furfural and after a 10x dilution by weight in water using a HPLC (Series 1500，Alltech，USA) with an Aminex HPX-87H column (Bio-Rad) and an 2.5 mM H_2SO_4 aqueous mobile phase flowing at 0.5 ml/min. HPLC systems were equipped with an RI detector (RI2000，Schambeck SFD GmbH，Germany). Concentrations of sugars were measured using the RI detector, while concentrations of 5-HMF and furfural were measured at 254 nm.

Oligomers contents were measured by HPLC. Briefly, hydrolysate solutions were analyzed for glucose and xylose before being placed in unstirred 15 ml thick-walled glass reactors (P160001，Beijing Synthware Glass Instrument Co., Ltd.，China).

The reactors were placed in an oil bath set to 120 °C for 60 min to hydrolyze any oligomers (i.e., gluco- and xylo-oligomers with degrees of polymerization > 1) to glucose and xylose. The hydrolysate solution was then re-analyzed for glucose and xylose, with the difference between the concentrations of the first and second analyses being defined as the oligomer concentration.

Supplementary Text

Irradiation assisted self-catalysis (IASC) in 40:60 GVL/H_2O solutions

Irradiation treatment prior to hydrolysis not only can disrupt the stubborn structure of lignocellulose (20), but also irradiation-mediated carboxylic acid, lactone, and phenol functional groups on the surface of biomass can act as catalytically active sites for (hemi) cellulose cleavages in 40:60 GVL/H_2O and the subsequent hydrolysis of carbohydrates to soluble sugars. FTIR and XPS spectra of (hemi) cellulose after irradiation treatment confirmed the formation of aforementioned groups, which results are in accordance with the changing trend of acid amount determined by acid–base titration (Fig. S18). The polar carboxyl groups are acting as “molecular radiators” in intermolecular of biomass, initiating the cleavage of the polysaccharide chain and selective formation of glucose (19). It has been demonstrated that the generated acid sites can cleave the β-1, 4-glyosidic bonds involving water molecules (15, 34) and catalyze the subsequent hydrolysis of carbohydrates to monomeric- and oligo-sugars. Direct cleavage and hydrolysis of the link between hemicellulose and cellulose by generated acid sites mediated from irradiation treatment in 40:60 GVL/H_2O is realized as the conception of self-catalysis without an adscititious catalyst. In

comparison, dilute acid pretreatment of biomass is typically carried out with at least 0.5 to 2 wt. % H_2SO_4 or HCl (35, 36). Although recent excellent research is available on soluble carbohydrates production from biomass in 80:20 GVL/H_2O, those mixture solutions contain more GVL proportions (80 wt. %) and dilute acid (~0.05% H_2SO_4) (11). This promising proposal for lignocellulose fractionation at high solid biomass loadings of 40 wt. % without an adscititiou catalyst in green aqueous solvents is a cost-effective and eco-friendly process, which shows much prospect for industrial applications of lignocellulose biorefinery in the future.

References

(1) A. J. Ragauskas et al., Science, 2006, **311**, 484-489.

(2) F. H. Isikgor, C. R. Becer, Polymer Chem., 2015, **6**, 4497-4559.

(3) P. Anbarasan et al., Nature, 2012, **491**, 235-239,

(4) R. Rinaldi, Angew. Chem. Int. Ed., 2014, **53**, 8559-8560.

(5) X, Chen et al., Energy Environ. Sci., 2016, **9**, 1237-1245.

(6) T. Y. Nguyen, C. M. Cai, O. Osman, R. Kumar and C. E. Wyman, Green Chem., 2015, **18**, 1581-1589.

(7) W. Zhao, R. Yang, Y. Zhang and L. Wu, Green Chem., 2012, **14**, 3352-3360.

(8) C. A. Cuvilas and W. Yang, Energy Fuels, 2012, **26**, 6426-6431.

(9) A. M. da C. Lopes, K. G. João, E. Bogel-Łukasik, L. B. Roseiro,and R. Bogel-Łukasik, J. Agric. Food Chem., 2013, **61**, 7874-7882.

(10) L. Heap, A. Green, D. Brown, B. van Dongen and N. Turner, Catal. Sci. Technol., 2014, **4**, 2251-2259.

(11) J. S. Luterbacher et al., Science, 2014, **343**, 277-280.

(12) S. G. Wettstein, D. M. Alonso, Y. Chong, J. A. Dumesic, Energy Environ. Sci., 2012, **5**, 8199-8203.

(13) S. Chuetor, R. Luque, C. Barron, A. Solhy, X. Rouau and A. Barakat, Green Chem., 2015, **17**, 926-936.

(14) C. Tissot, S. Grdanovska, A. Barkatt, J. Silverman, M Al-Sheikhly, Rad. Phys. Chem., 2013, **84**, 185-190.

(15) M. Benoit et al., Angew. Chem. Int. Ed. Engl., 2011, **50**, 8964-8967.

(16) L. Zhou et al., Green Chem., 2015, 17, 1519-1524.

(17) P. M. Grande, J. Viell, N.s Theyssen, W. Marquardt, P. D. de María and W. Leitner, Green Chem., 2015, **17**, 3533-3539.

(18) W. Fang and H. Sixta, ChemSusChem., 2015, **8**, 73-76.

(19) A. T. To, P.-W. Chung, and A. Katz, Angew. Chem. Int. Ed., 2015, **54**, 11050-11053.

(20) Y. Liu, H. Zhou, L. Wang, S. Wang, L. Fan, Chem. Eng. J., 2016, **287**, 302-312.

(21) F. K. Kazi et al., Fuel, 2010, **89**, S20-S28.

(22) Y. J. Pagán-Torres, T. Wang, J. M. R. Gallo, B. H. Shanks, J. A. Dumesic, ACS Catal., 2012, **2**, 930-934.

(23) E. I. Gürbüz et al., Angew. Chem. Int. Ed. Engl., 2013, **52**, 1270-274.

(24) D. M. Alonso, S. G. Wettstein, M. A. Mellmer, E. I. Gurbuz and J. A. Dumesic, Energy Environ. Sci., 2013, 6, 76-80.

(25) M. A. Mellmer et al., Angew. Chem. Int. Ed. 2014, **53**, 11872-11875.

(26) Z. Liu, Y. Gao, J. Chen, T. Imanaka, J. Ba, Q. Hua, Bioresoure Technol., 2013, **130**, 144-151.

(27) Y. Qian, Y. Deng, X. Qiu, H. Li and D. Yang, Green Chem., 2014, **16**, 2156-2163.

(28) A. P. Richter et al., Nature Nanotechnol., 2015, **10**, 817-825.

(29) R. Katahira, et al., ACS Sustainable Chem. Eng., 2016, **4**, 1474−1486.

(30) A. Rahimi, A. Ulbrich, J. J. Coon & S. S. Stahl, Nature, 2014, **515**, 249-252.

(31) A. Rahimi, A. Azarpira, H. Kim, J. Ralph and S. S. Stahl, J. Am. Chem. Soc., 2013, **135**, 6415-6418.

(32) L. da C. Sousa, et al., Energy Environ. Sci., 2016, **9**, 1215-1223.

(33) Z. Gong, Q. Wang, H. Shen, C. Hu, G. Jin, Z. K. Zhao, Bioresoure Technol., 2012, **117**, 20-24.

(34) J. Fan et al., J. Am. Chem. Soc., 2013, **135**, 11728-11731.

(35) N. Mosier et al., Bioresoure Technol., 2005, **96**, 673-686.

(36) M.V. Bule, A.H. Gao, B. Hiscox, S. Chen, J. Agr. Food Chem., 2013, **61**, 3916-3925.

Table S1 Compositions of tested lignocelluloses of reed stover, corncob, bagasse, eucalyptus and pine

Compositions	Agricultural waste biomass						Plant woods			
	Untreated or native			Irradiation treatment			Untreated or native		Irradiation treatment	
	Reed stover	Corncob	Bagasse	Reed stover	Corncob	Bagasse	Eucalyptus	Pine	Eucalyptus	Pine
Cellulose / %	38.87	33.85	38.06	37.33	26.97	29.23	41.27	38.66	32.63	32.46
Hemicellulose / %	18.99	26.78	25.53	17.14	26.25	25.10	15.28	19.14	14.28	18.69
Lignin / %	23.28	11.06	9.02	20.25	15.55	12.54	26.61	26.48	30.65	29.74
Acetyl / %	3.02	4.15	8.89	2.87	3.68	6.78	4.53	3.42	4.20	3.05
Ash / %	1.55	2.73	2.74	1.00	2.28	2.58	2.12	2.81	1.75	1.05

Note: cellulose content is calculated as glucan content; hemicellulose content is expressed as xylan content; Lignin content is represented as acid insoluble lignin content.

Table S2 The IR absorbance of characteristic peak and soluble sugars in irradiated and native samples.

Feed stocks	Acid amount ($mmol.g^{-1}$)	FT-IR Absorbance of C=O			Water soluble glucose oligomers($mg.g^{-1}$)	Water soluble xylose oligomers($mg.g^{-1}$)
		λ^{a}($1605cm^{-1}$)	λ^{b}($1633cm^{-1}$)	λ^{c}($1733cm^{-1}$)		
Native sample	0.04	0.17	0.15	0.11	2.64	4.36
Irradiated sample	0.28	0.31	0.25	0.28	25.27	44.60

λ^{a} C=O stretching and aromatic vibrations; S > G; condensed G > etherified G; λ^{b} C=O stretching vibrations, characteristics of para-substituted aryl skeleton; λ^{c} carbonyl stretch in unconjugated ketones and carboxylic groups [34]

Table S3 Gel-permeation chromatographic (GPC) analysis of different lignin.

Lignin type	**M_n (g mol^{-1})**	**M_w (g mol^{-1})**	**PI**
EHL[a]	1967	3053	1.55
IASC-Lignin[b]	1410	1664	1.18

EHL: enzymatic hydrolyzed lignin; IASC: irradiation assisted self-catalysis. PI: polydispersity index; [a] enzymatic hydrolyzed lignin from native reed stover; [b] lignin from irradiation assisted self-catalysis fractionation process at 170 ^{o}C, 1 h, GVL:H_2O=4:6, 18 wt. % solids loading.

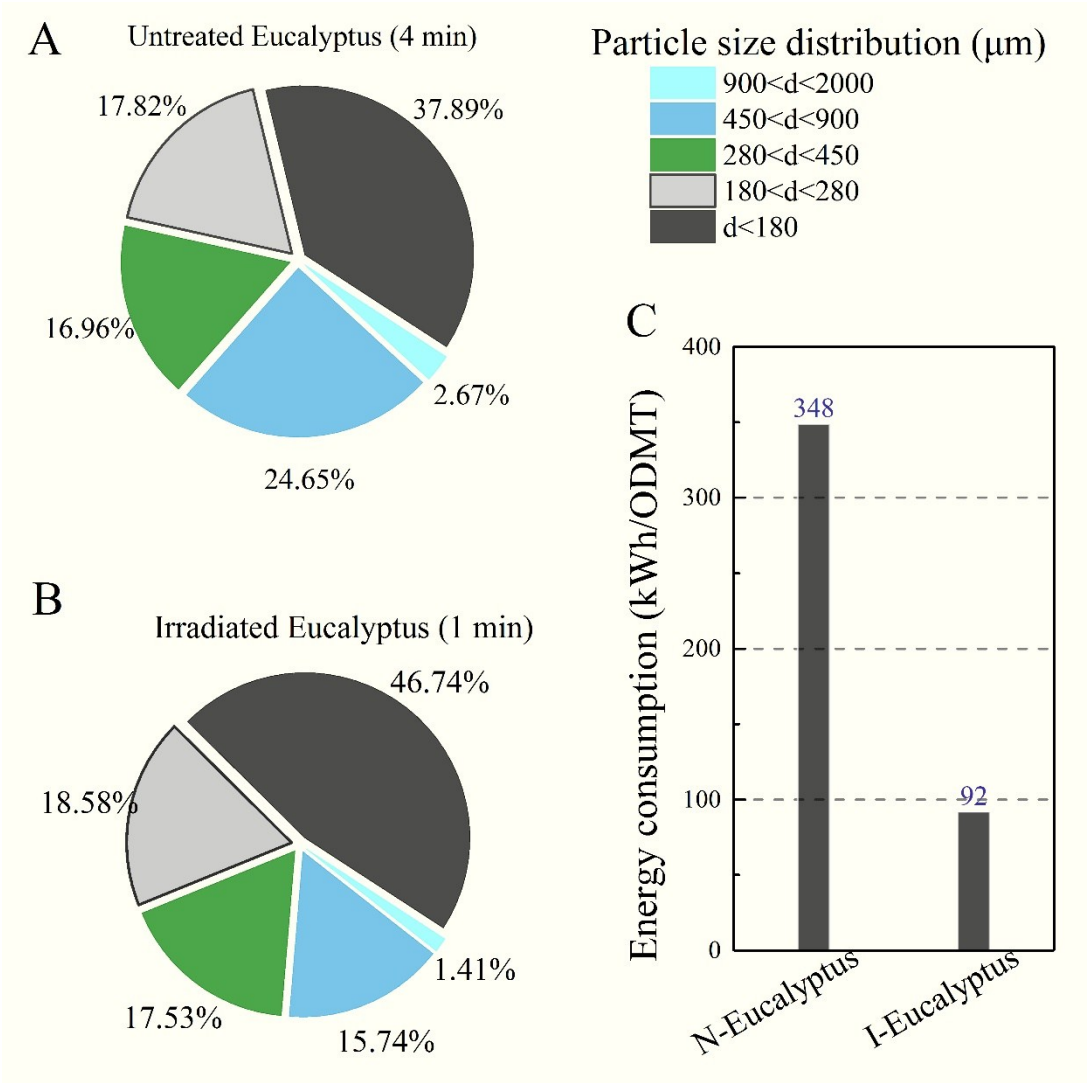

Fig. S1 Comparisons of particle size distributions and energy consumption of grinding irradiated and untreated Eucalyptus. (A) particle size distributions of untreated Eucalyptus, after 4 min grinding; (B) particle size distributions of irradiated Eucalyptus, after 1 min grinding; (C) energy consumption of grinding irradiated and untreated Eucalyptus; N-Eucalyptus: native Eucalyptus material; I-Eucalyptus: irradiated Eucalyptus material.

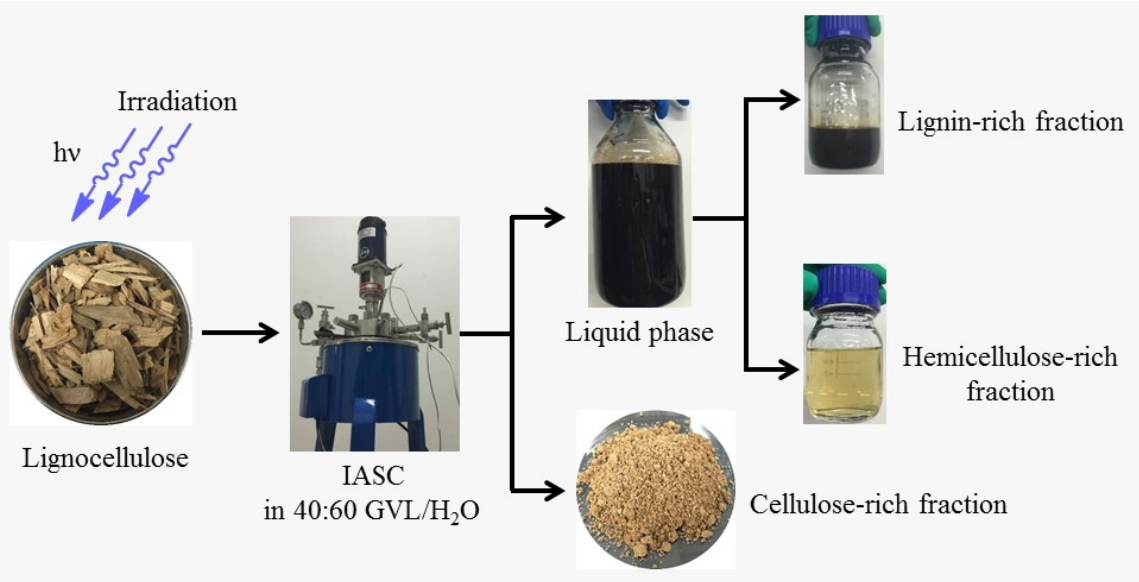

Fig. S2 Schematic representation of (hemi) cellulose- and lignin-rich fractionation from biomass through IASC in 40:60 GVL/H_2O green solvent aqueous mixture solvents

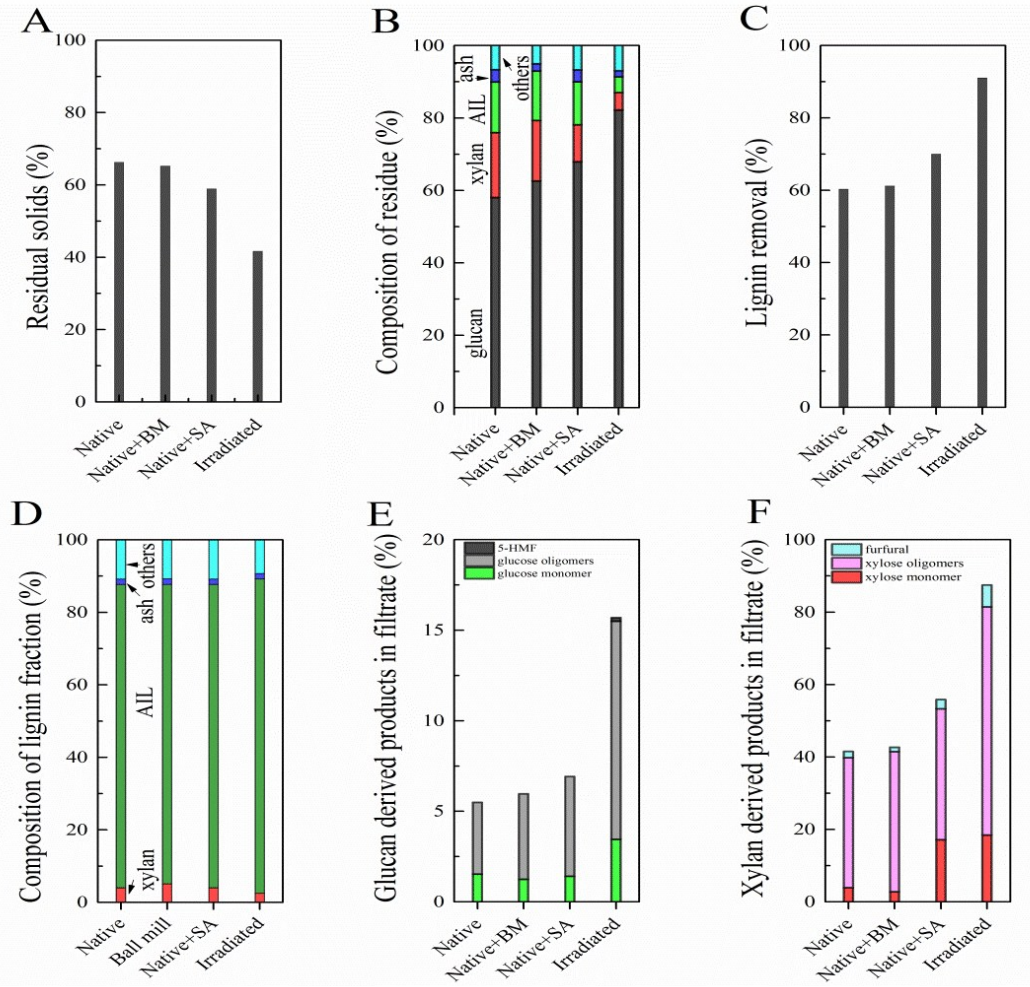

Fig. S3 Effect of different treatment methods, including IASC, adding mineral acid as catalyst, and ball-milling, on the biomass fractionation in 40:60 GVL/H_2O at 170 °C for 1 h. Native indicates untreated biomass as the reference. BM means ball-milling treatment. SA represents for adding sulfuric acid as catalyst. Irradiation stands for irradiation-assisted self-catalysis treatment.

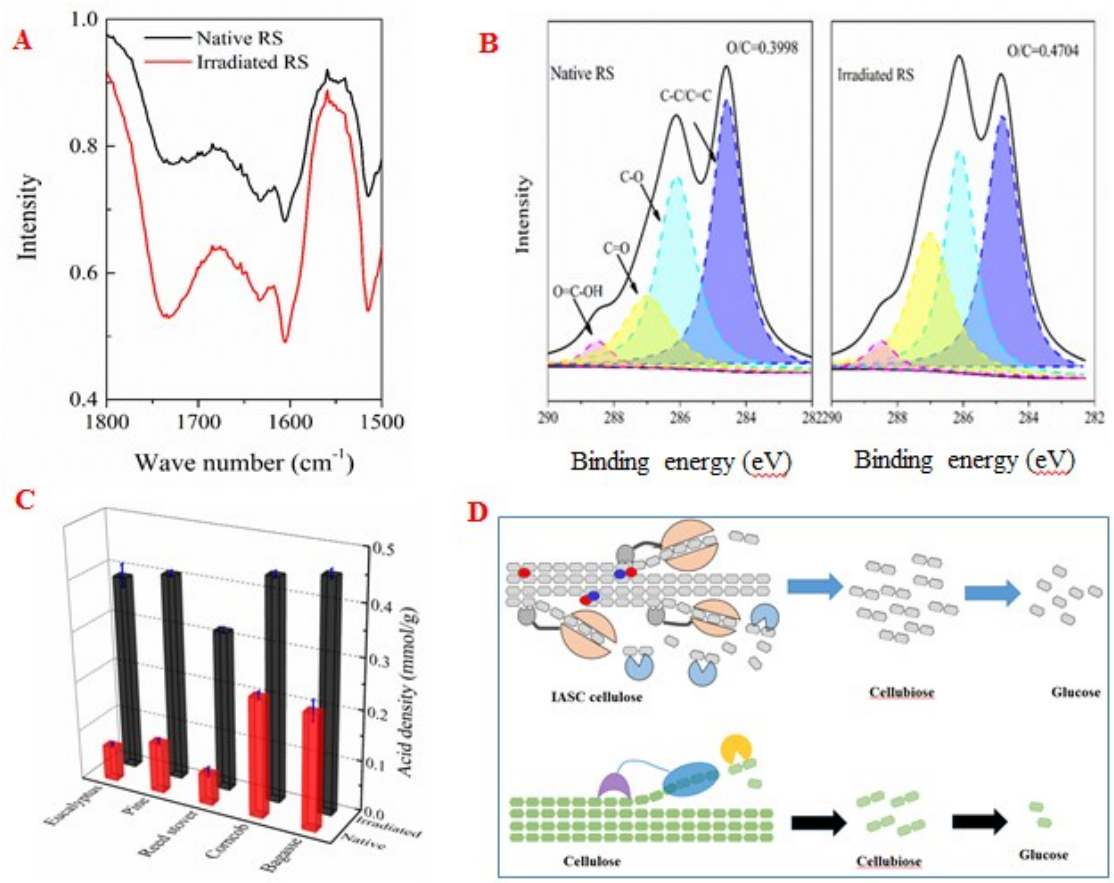

Fig. S4 The mechanism for high enzymatic saccharification efficiency of cellulose obtained through IASC in 40:60 GVL/H_2O. (A) FT-IR spectra of biomass before and after irradiation treatment; (B) XPS spectra of biomass before and after irradiation treatment; (C Acid-base titration for the measurement of acid density content of biomass before and after irradiation treatment; (D) The key for overall efficiency of the synergistic impacts of catalytic acid sites on cellulose surface mediated from irradiation oxidation and adsorption capacity of cellobiohydrolase (CBH).

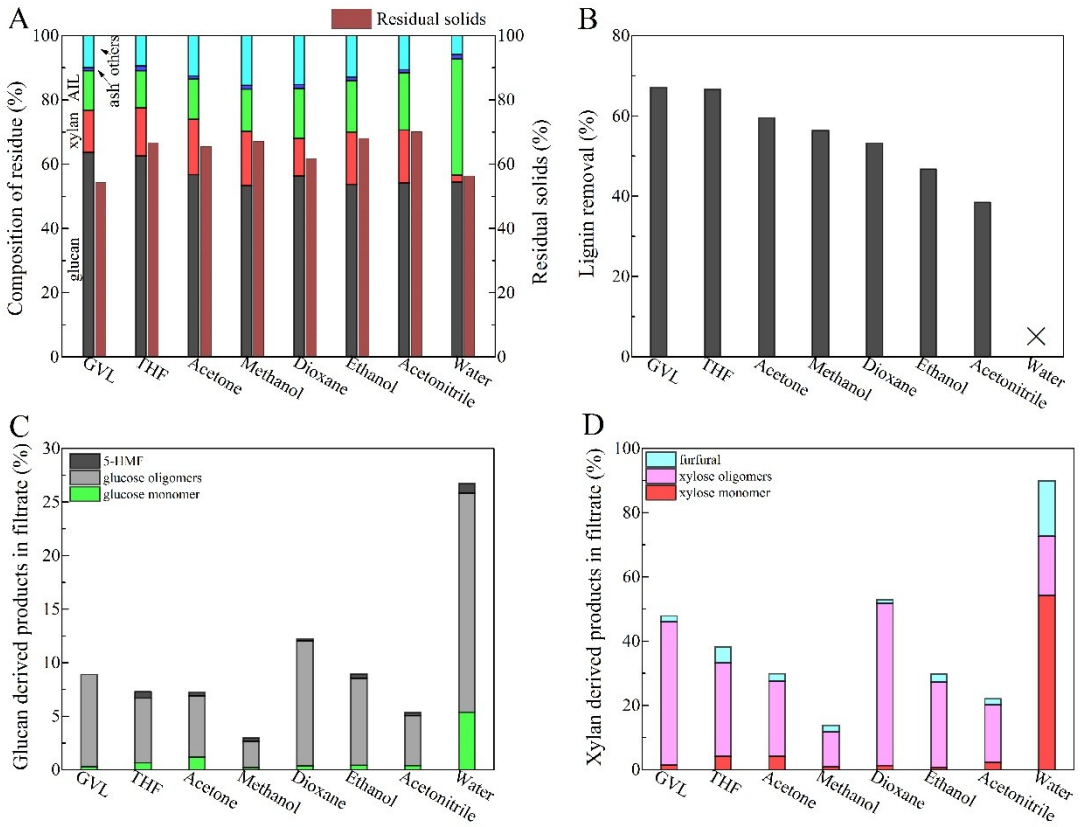

Fig. S5 The different fractionation efficiency through IASC in seven different solvent aqueous systems at 170 °C for 2 h. Weight ratio of solvent to water is fixed at 80:20.

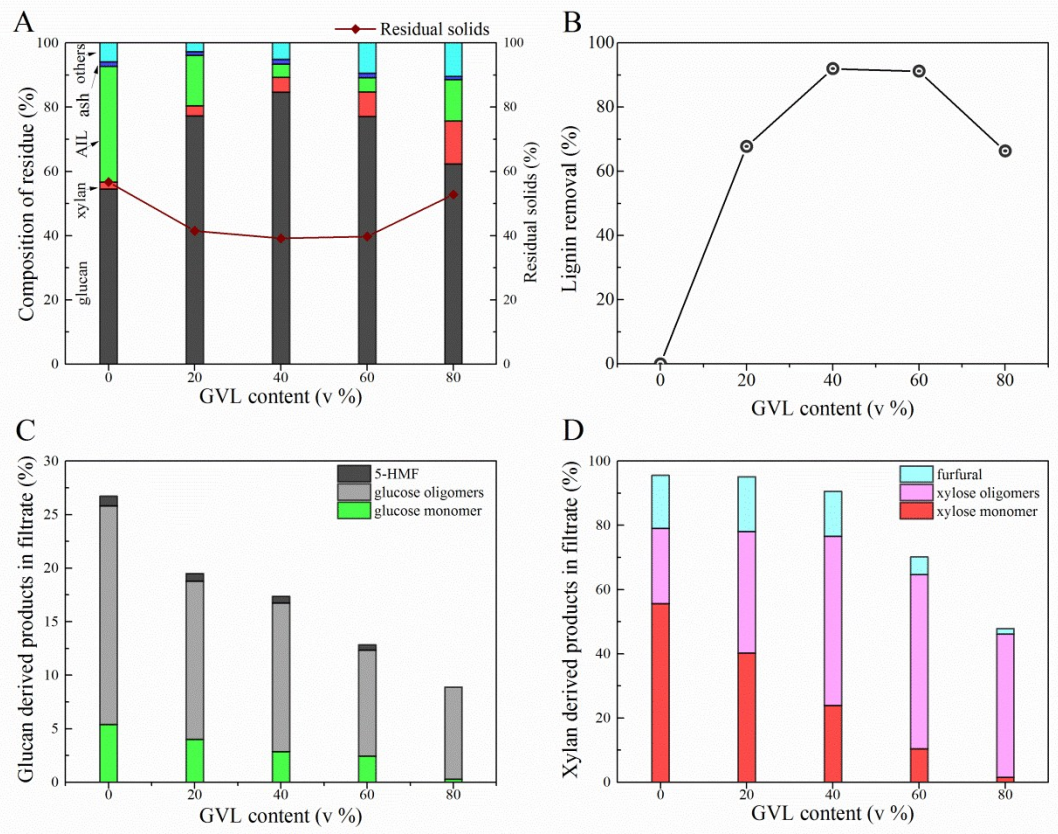

Fig. S6 Lignocellulose fractionation efficiency through IASC in GVL/H_2O at 170 °C for 2 h as the functions of weight ratios of solvent to water from 20 wt.% to 80 wt.%

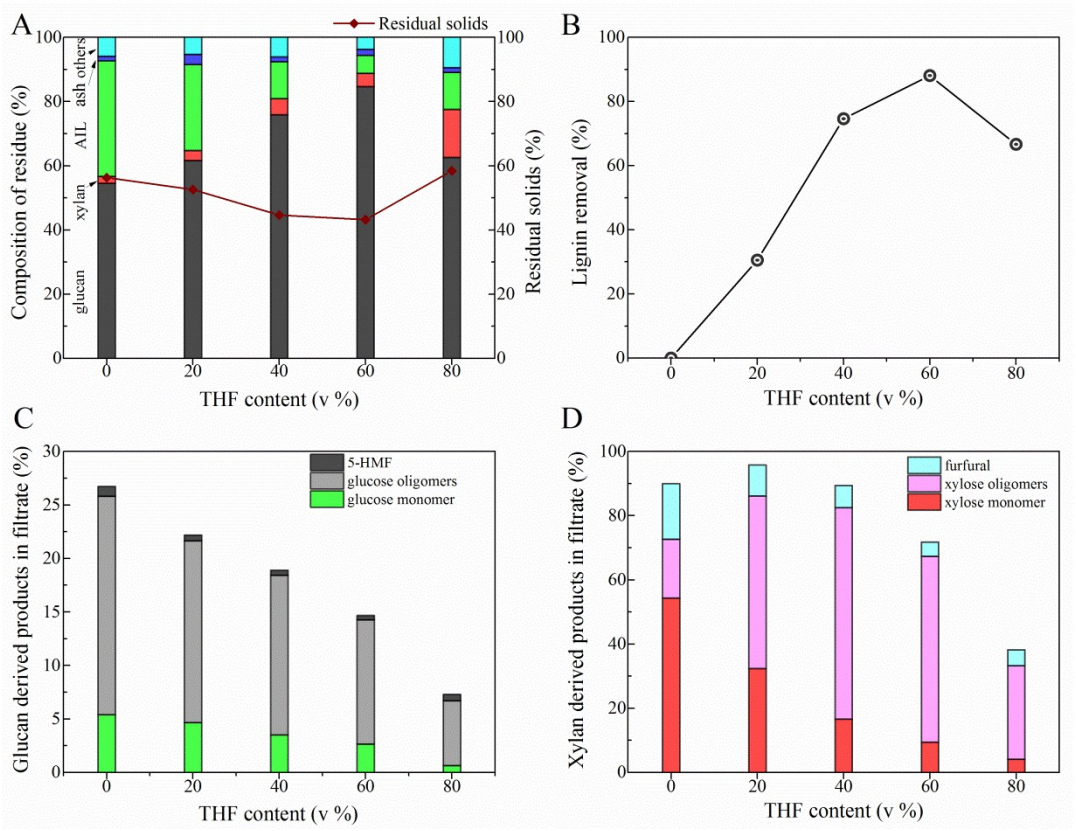

Fig. S7 Lignocellulose fractionation efficiency through IASC in THF/H_2O at 170 °C for 2 h as the functions of weight ratios of solvent to water from 20 wt.% to 80 wt.%

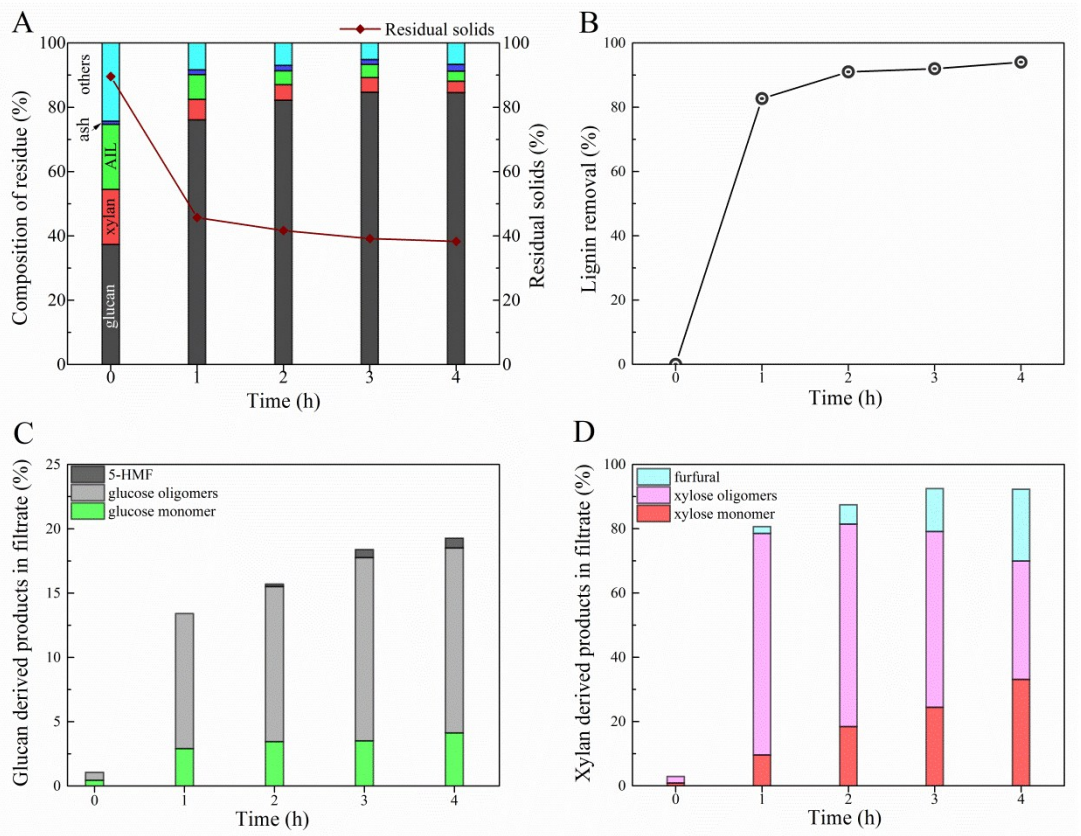

Fig. S8 The kinetic curve of biomass fractionation as the functions of reaction time through IASC in 40:60 GVL/H_2O at 170 °C, 10 wt. % solids loading.

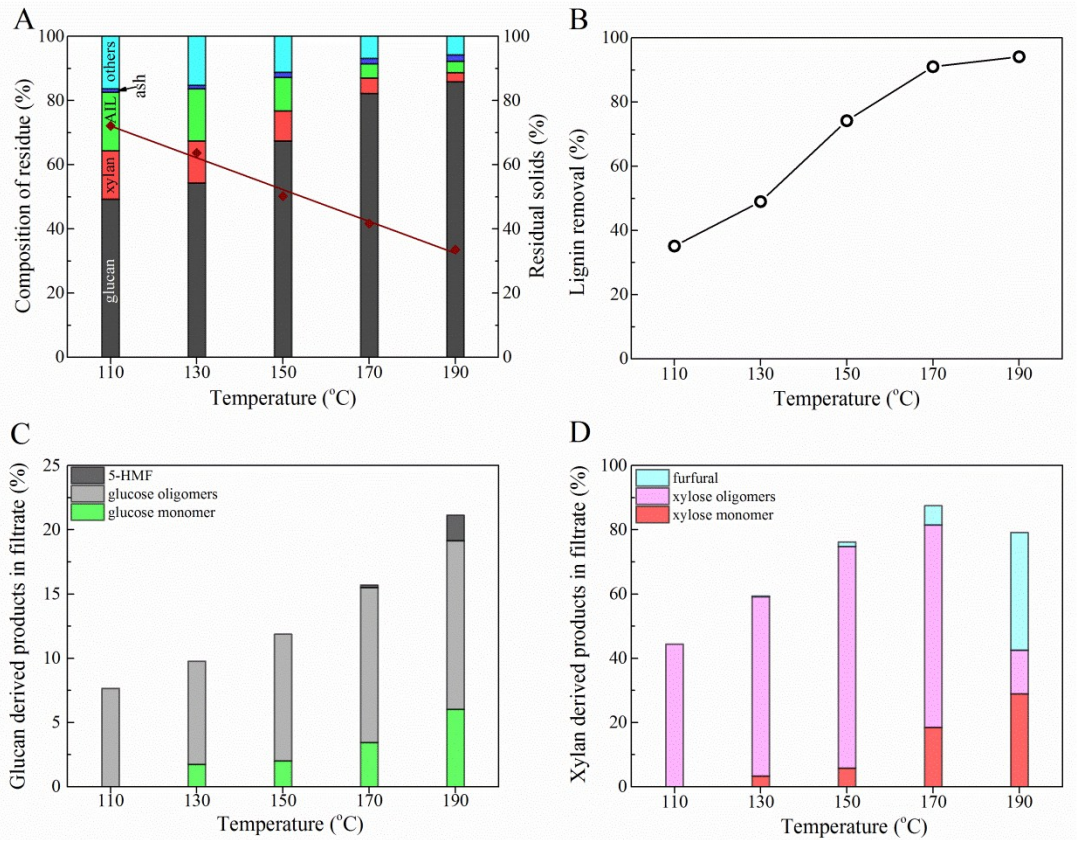

Fig. S9 The biomass fractionation as the functions of reaction temperatures ranging from 110- 190 °C through IASC in the 40:60 GVL/H_2O for 2 h, 10 wt. % solids loading.

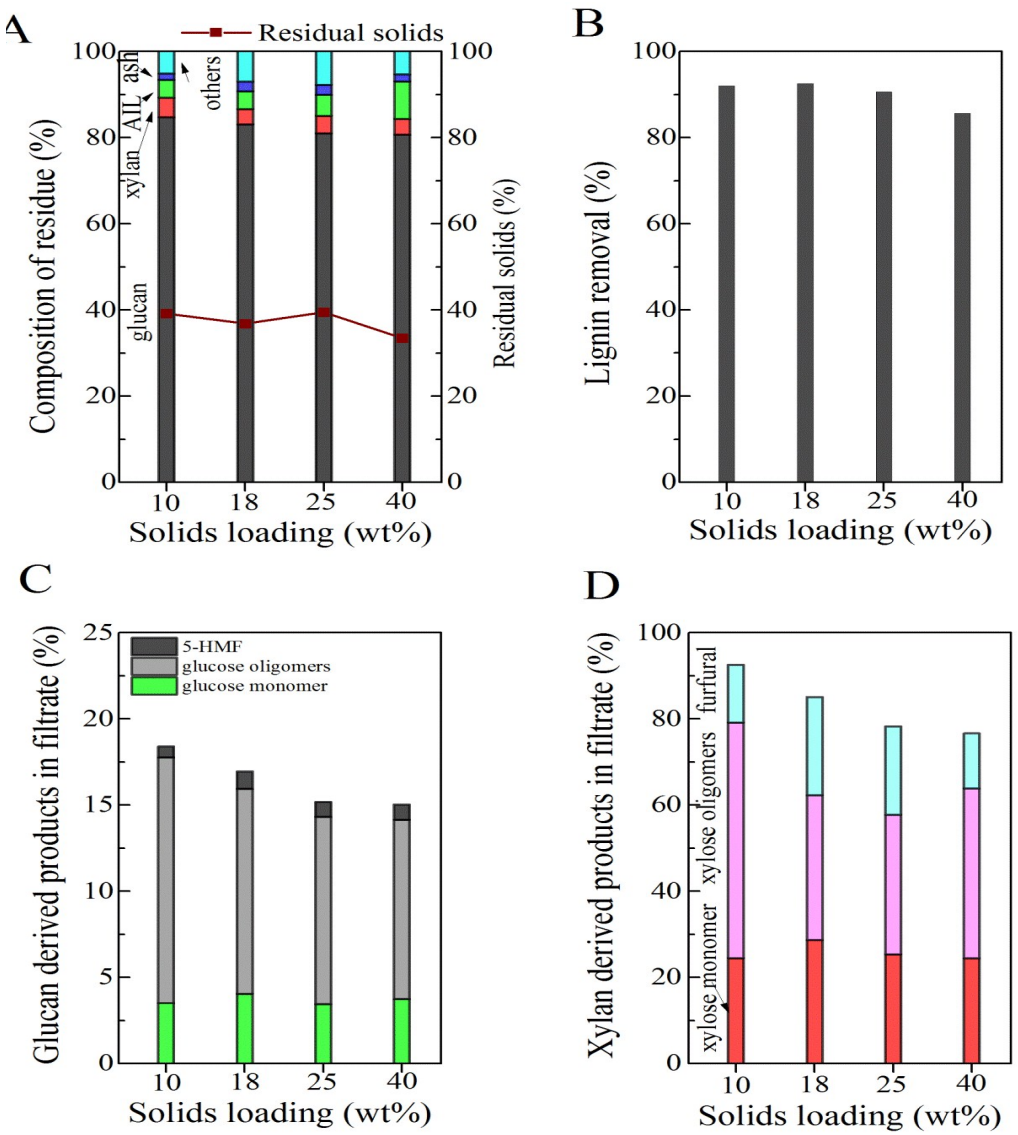

Fig. S10 The effect of biomass loadings on fractionation through IASC in the 40:60 GVL/H_2O at 170 °C for 1 h

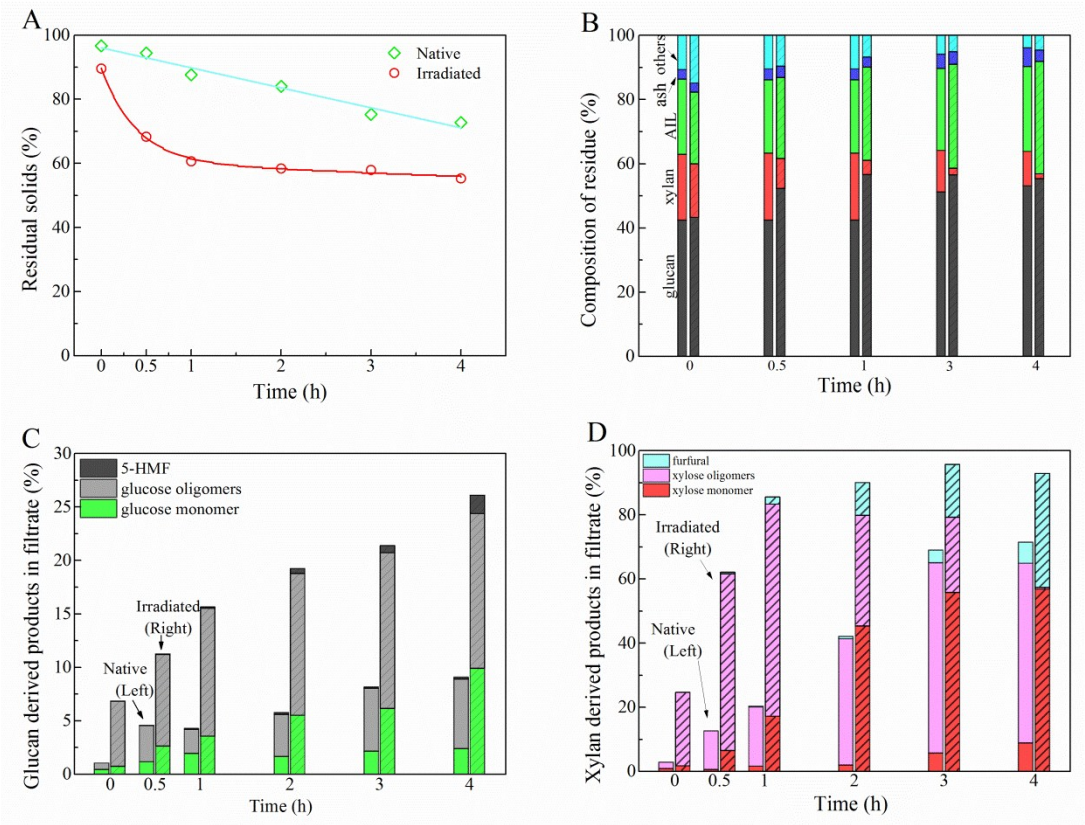

Fig. S11 The kinetic curve of biomass fractionation as the functions of reaction time through IASC in water instead of organic solvent at 170 °C

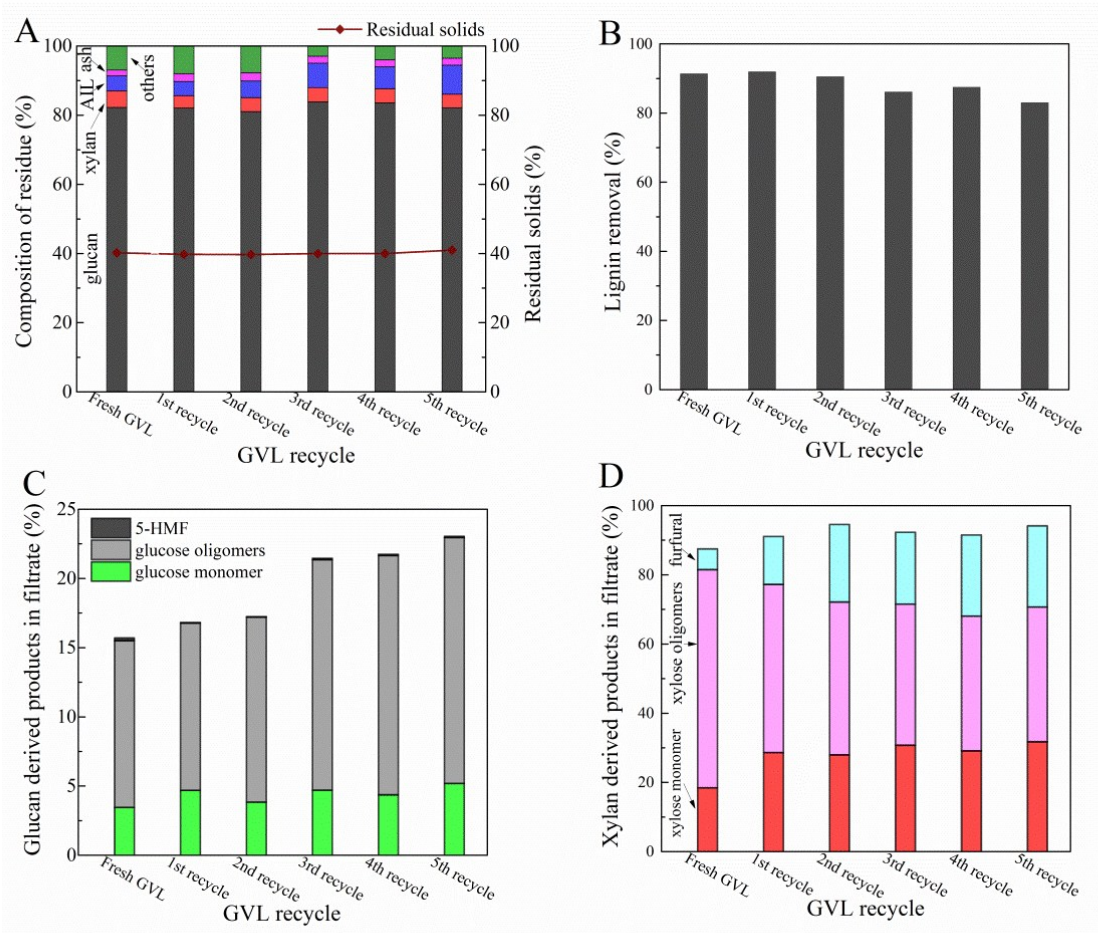

Fig. S12 Effect of GVL recycles on biomass fractionation through IASC in 40:60 GVL/H_2O at 170 °C for 1 h

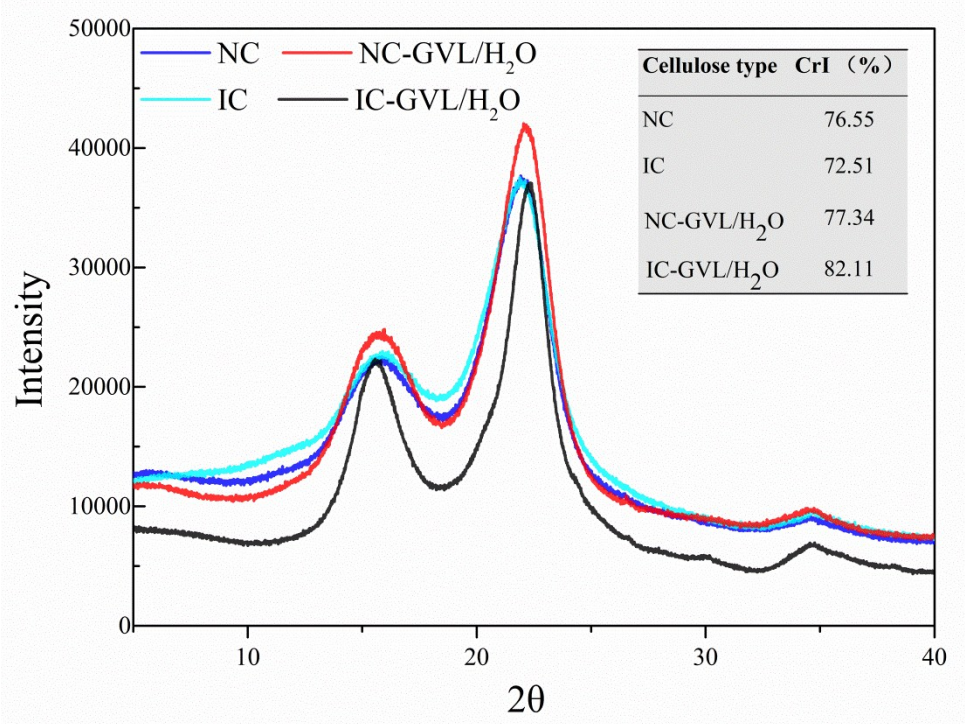

Fig. S13 XRD images and crystallinity indexes (Crl) of native cellulose of reed stover (NC), irradiated cellulose of reed stover (IC), cellulose fraction of native reed stover isolated from 40:60 GVL/H_2O (NC-GVL/H_2O), and cellulose fraction isolated from IASC in 40:60 GVL/H_2O (IC-GVL/H_2O).

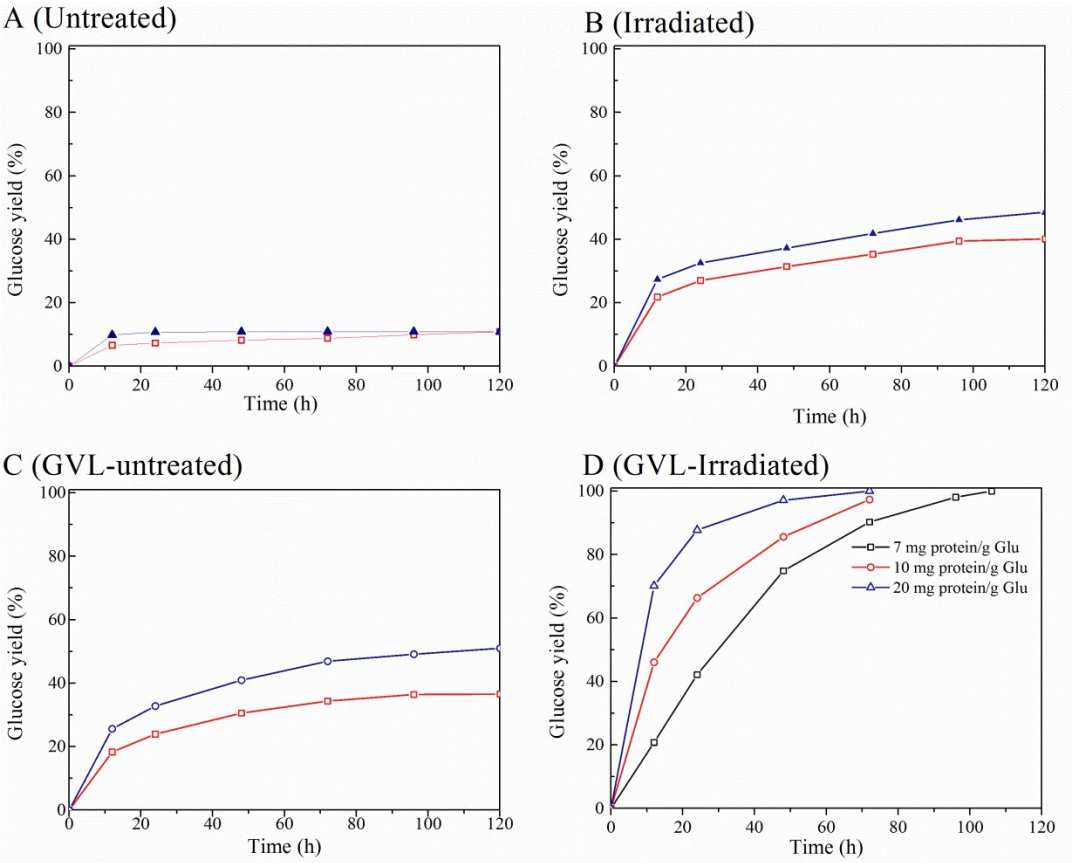

Fig. S14 Effect of enzyme loadings on enzymatic hydrolysis of cellulose-rich fraction obtained by different operational units, including from native biomass, irradiated biomass, GVL extracted biomass, and biomass treated irradiation in 40:60 GVL/H_2O

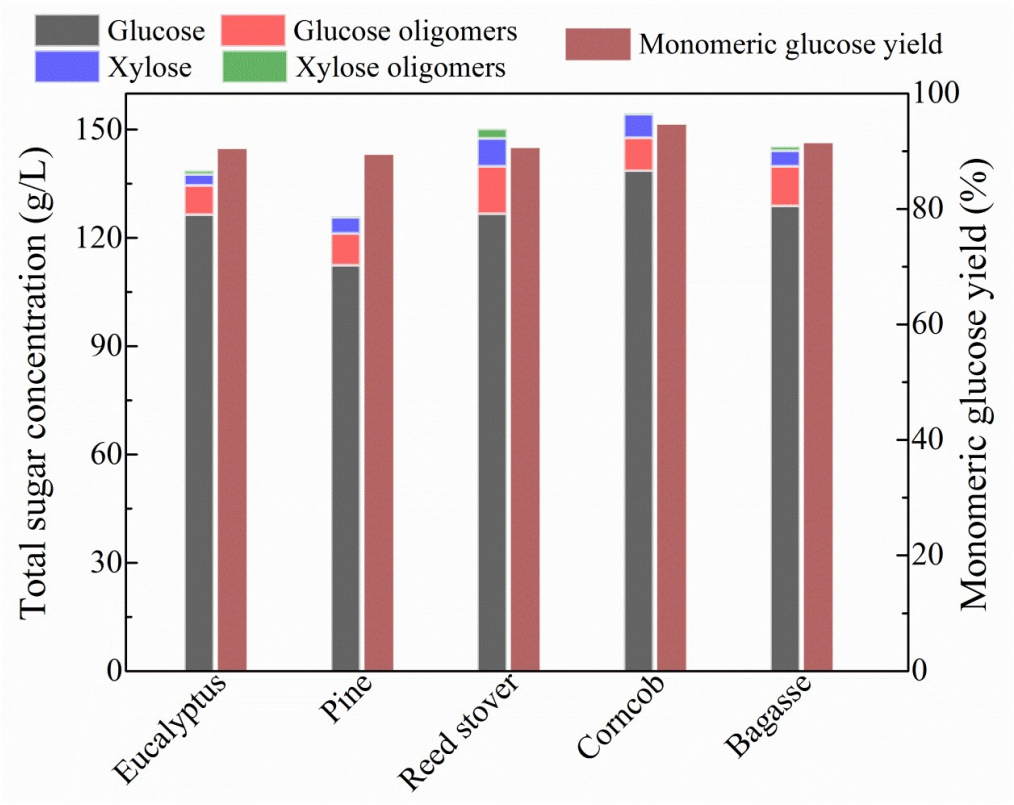

Fig. S15 The yields of total soluble sugars and monomeric glucose by enzymatic hydrolysis (10 mg protein per g cellulose) for different celluloses from different kinds of biomass fractionation through IASC in 40:60 GVL/H_2O at 170 °C for 1 h.

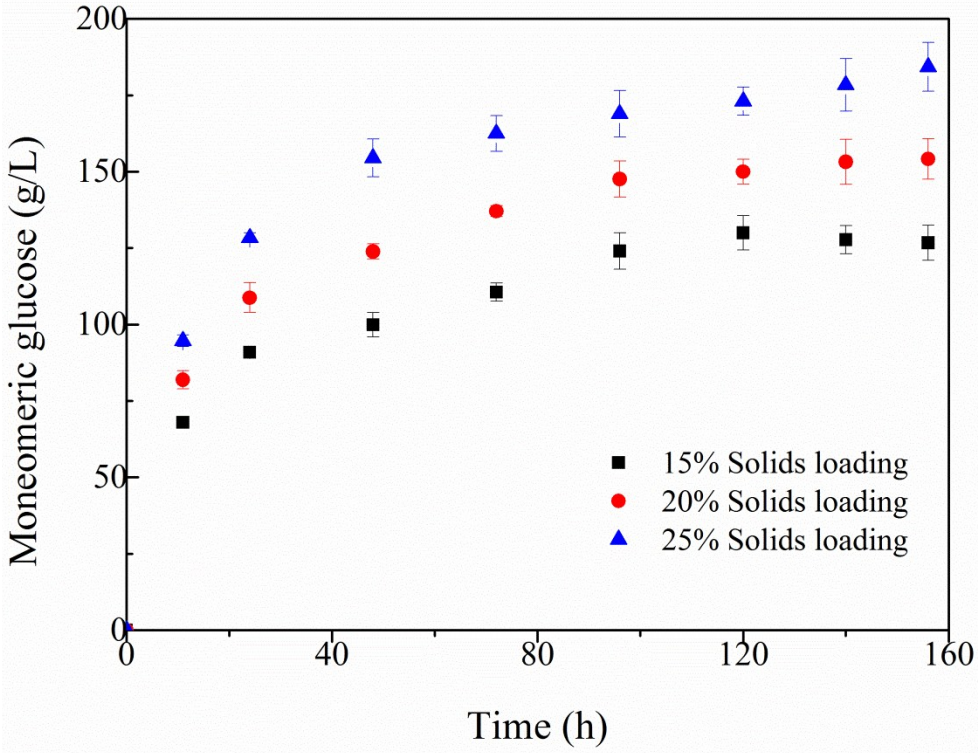

Fig. S16 The effects of cellulose loadings on the yields of monomeric glucose when it is fixed the enzymes loadings at 20 mg protein per g cellulose.

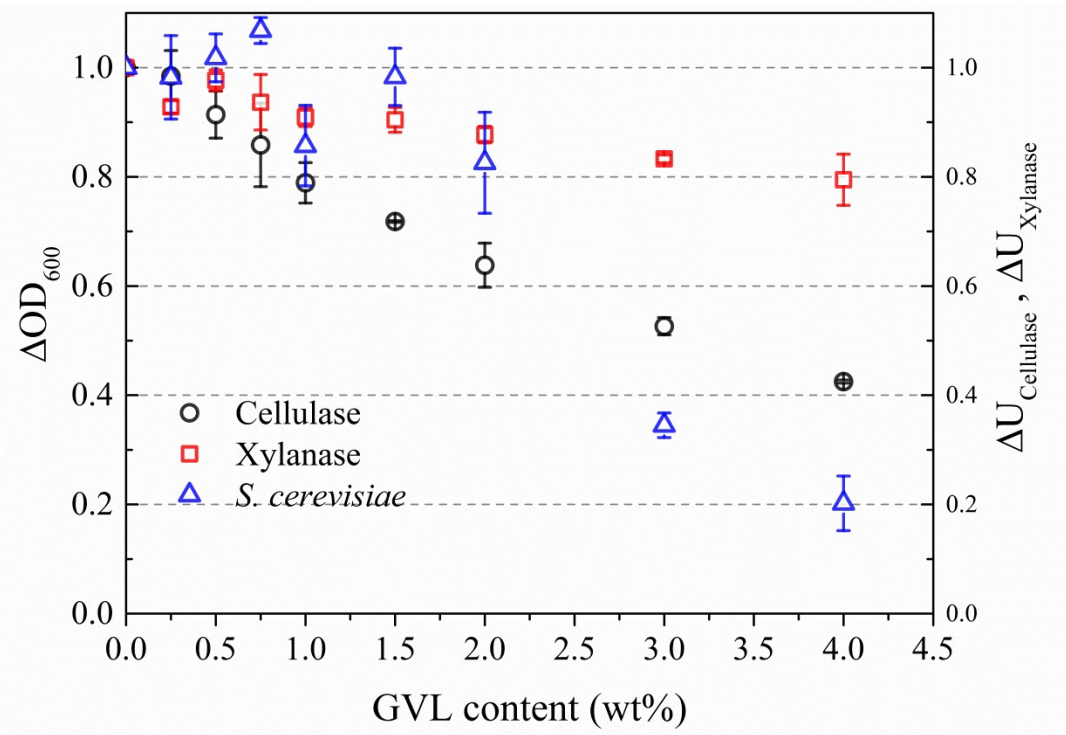

Fig. S17 Effect of GVL content ranging from 0 wt. % to 4.0 wt. % retained in cellulose residue on enzyme activities and *S. cerevisie* growth.

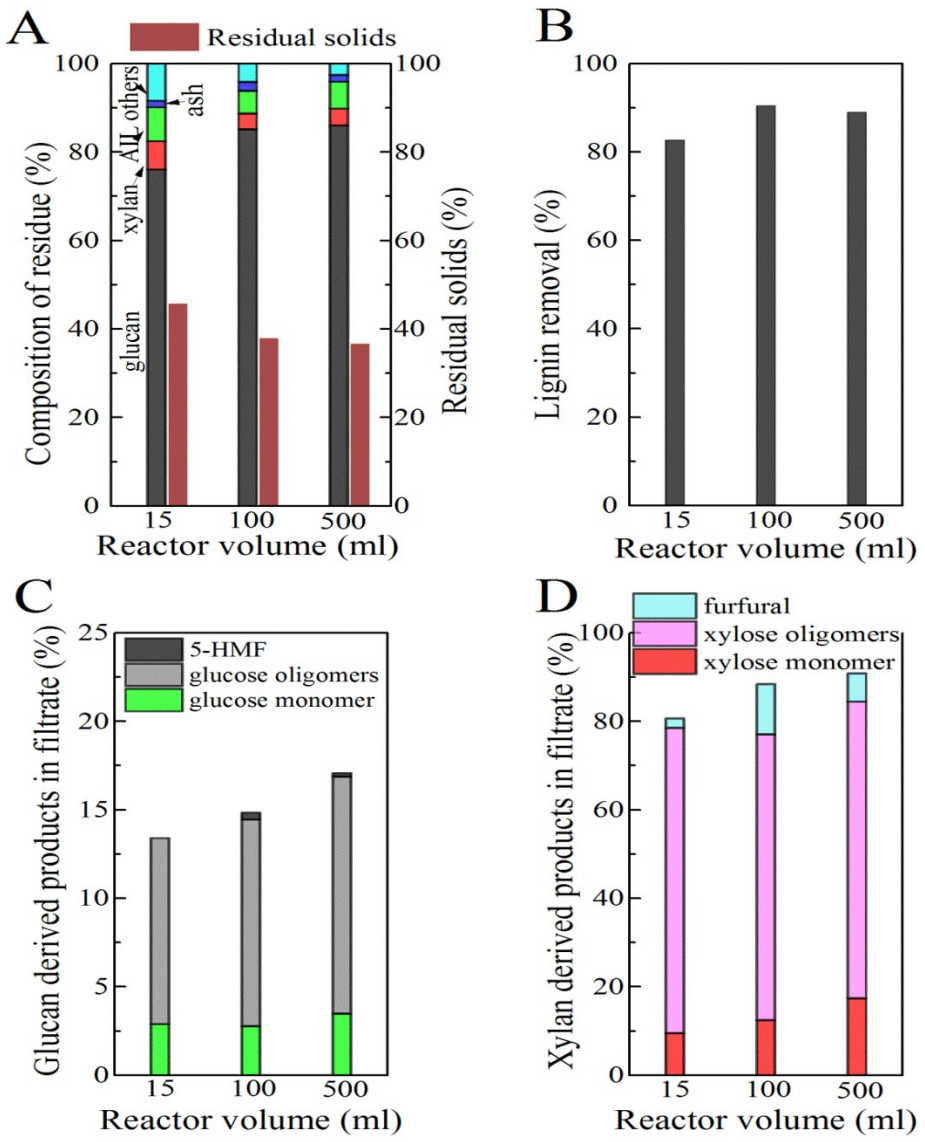

Fig. S18 Biomass fractionation in 15 mL-100 mL-500mL laboratory-scale reactors with 17 wt. % biomass loadings through IASC in 40:60 GVL/H_2O at 170 °C for 1 h.